Supplementary Information

Silica nanoparticles drive disease-suppressive microbiome assembly via inosine-associated metabolic reprogramming and biofilm promotion

Minghao Lv[1,2,6#], Wenchong Shi[1,2,5#*], Shidong He[1,2], Yang Li[1,2], Mingcong Li[1,2,4], Yanyan Zhou[1,2], Lanxiang Ma[7], Jie Xu[7], Fengjie Nie[8], Tangyuan Ning[1,3*], Bo Zhou[1,2,4*], Zheng Gao[1,2,4,5*]

[1] *State Key Laboratory of Wheat Improvement, Shandong Agricultural University, Tai'an 271018, Shandong, China*

[2] *College of Life Sciences, Shandong Agricultural University, Tai'an 271018, Shandong, China*

[3] *College of Agronomy, Shandong Agricultural University, Tai'an 271018, Shandong, China*

[4] *Shandong Engineering Research Center of Plant-Microbe Restoration for Saline-Alkali Land, Shandong Agricultural University, Tai'an 271018, Shandong, China*

[5] *Shandong Bohua High-Efficiency Ecological Agriculture and Technology Co., Ltd., Binzhou 256506, Shandong, China*

[6] *Institute of Ecology, State Key Laboratory of Vegetation Structure, Function and Construction (VegLab), and College of Urban and Environmental Sciences, Peking University, Beijing 100000, China*

[7] *Zaozhuang Academy of Agricultural Sciences, Zaozhuang 277000, Shandong, China*

[8] *Ningxia Academy of Agriculture and Forestry Sciences, Agricultural Biotechnology Research Center, Yinchuan 750000, Ningxia, China*

[#] These authors contributed equally to this work.

[*]Address correspondence to Zheng Gao (email: gaozheng@sdau.edu.cn); Bo Zhou (email: zhoubo2798@163.com); Tangyuan Ning (email: ningty@163.com); or Wenchong Shi (email: shiwenchong@sdau.edu.cn)

The supplementary information includes the following:

Figures S1-S15

Legends for Tables S1-S8

Legends for Tables S1-S8

Table S1. Statistical results of field trials with SiO_2 NP treatments.

Table S2. ANI and dDDH values between strains PH3-11 and FZB42.

Table S3. Genomic features of strain PH3-11.

Table S4. Prophage prediction information of PH3-11.

Table S5. antiSMASH prediction of secondary metabolite biosynthetic gene clusters in strain PH3-11.

Table S6. Differences in relative isovaleric acid levels.

Table S7. Statistical results of field trials with PH3-11, inosine, and synbiotic treatments.

Table S8. Differential expression of PH3-11 genes.

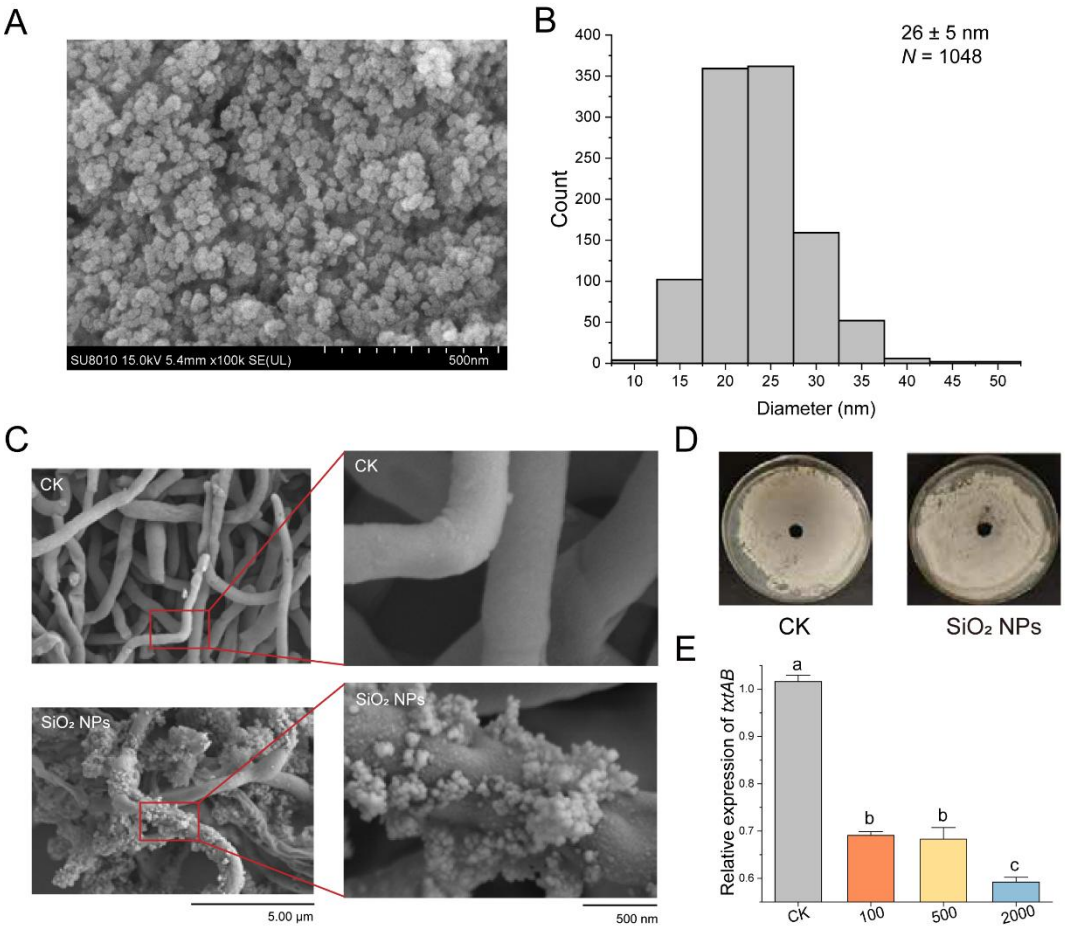

Figure S1. Characterization of SiO_2 NPs and their direct effects on the potato common scab pathogen. (A) Representative SEM image of the SiO_2 NPs. (B) Particle size distribution based on SEM image analysis. (C) Scanning electron micrographs of the pathogen after treatment with SiO_2 NPs. (D) Agar plate assay evaluating the direct inhibitory effect of SiO_2 NPs on the pathogen. (E) Effect of SiO_2 NPs on the expression of the thaxtomin biosynthesis genes *txtAB* in the pathogen. In panel E, different letters indicate significant differences among treatments at $P < 0.05$, as determined by one-way ANOVA followed by Duncan's multiple range test.

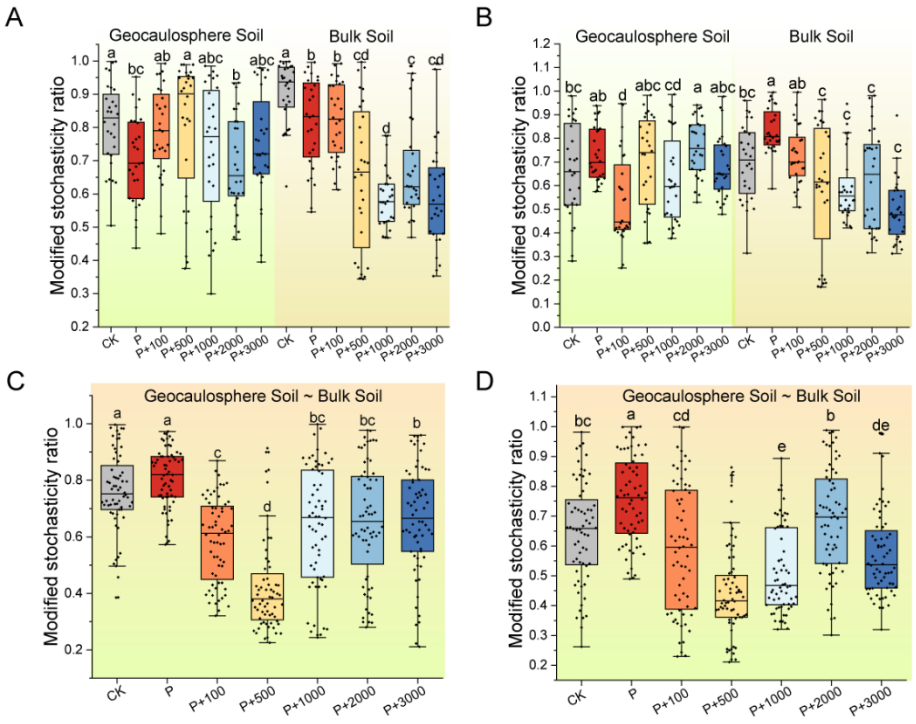

Figure S2. Modified stochasticity ratio (MST) of soil microbial communities under different SiO_2 NP treatments. (A) MST of bacterial communities in geocaulosphere soil and bulk soil. (B) MST of fungal communities in geocaulosphere soil and bulk soil. (C) MST of bacterial communities between geocaulosphere and bulk soil. (D) MST of fungal communities between geocaulosphere and bulk soil.

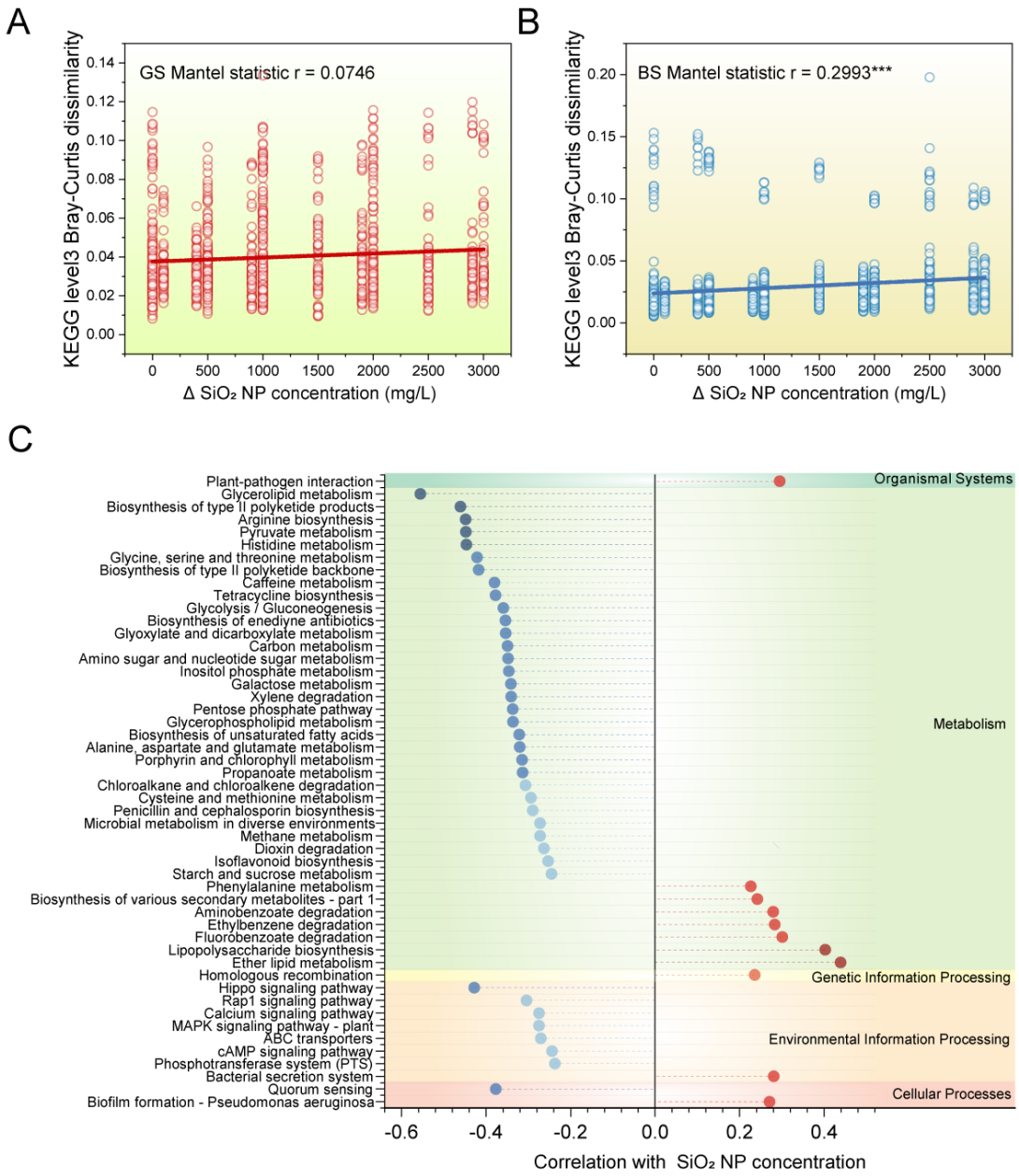

Figure S3. Functional prediction of soil bacterial communities. (A) Scatter plot of the correlation between differences in SiO_2 NP concentration and Bray–Curtis dissimilarity of bacterial community function in geocaulosphere soil. (B) Scatter plot of the correlation between differences in SiO_2 NP concentration and Bray–Curtis dissimilarity of bacterial community function in bulk soil. (C) Correlation between SiO_2 NP concentration and bacterial community function. $P < 0.05$ was considered statistically significant. Significance: *$P < 0.05$; **$P < 0.01$; ***$P < 0.001$.

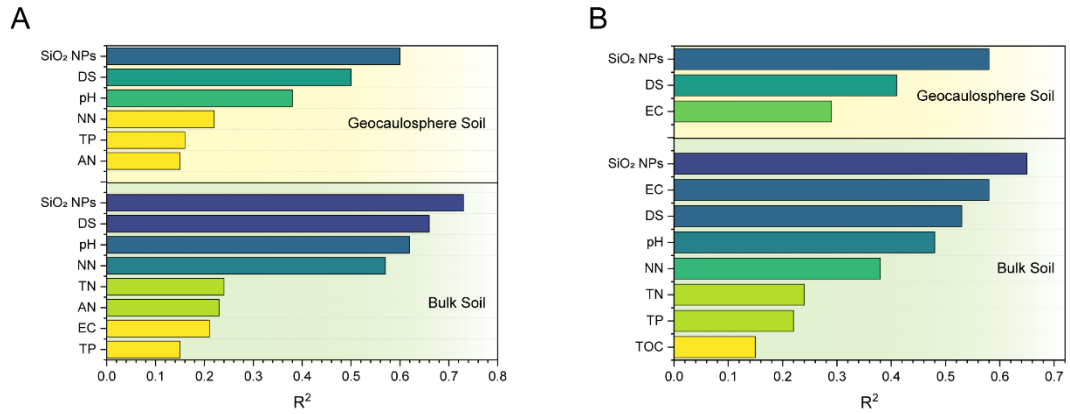

Figure S4. Redundancy analysis of soil microbial communities and environmental factors. (A) Redundancy analysis of bacterial communities and environmental factors. (B) Redundancy analysis of fungal communities and environmental factors. R^2 reflects the degree to which environmental factors explain changes in microbial community structure ($P < 0.05$). DS: disease severity; TN: total nitrogen; TP: total phosphorus; AN: ammonium nitrogen; NN: nitrate nitrogen; TOC: total organic carbon; EC: electrical conductivity.

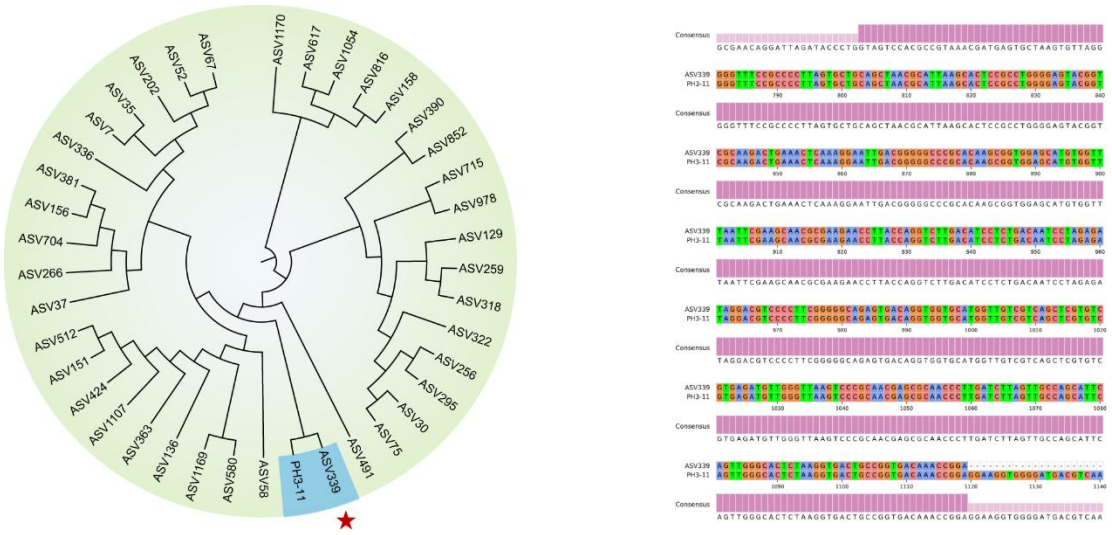

Figure S5. Phylogenetic relationships among candidate biocontrol ASVs and strain PH3-11. ASV339 is marked with a star. The sequence alignment shows that ASV339 shared 100% sequence identity with the corresponding amplified region of the PH3-11 16S rRNA gene.

Figure S6. Antagonistic activity of strain PH3-11 against the potato common scab pathogen.

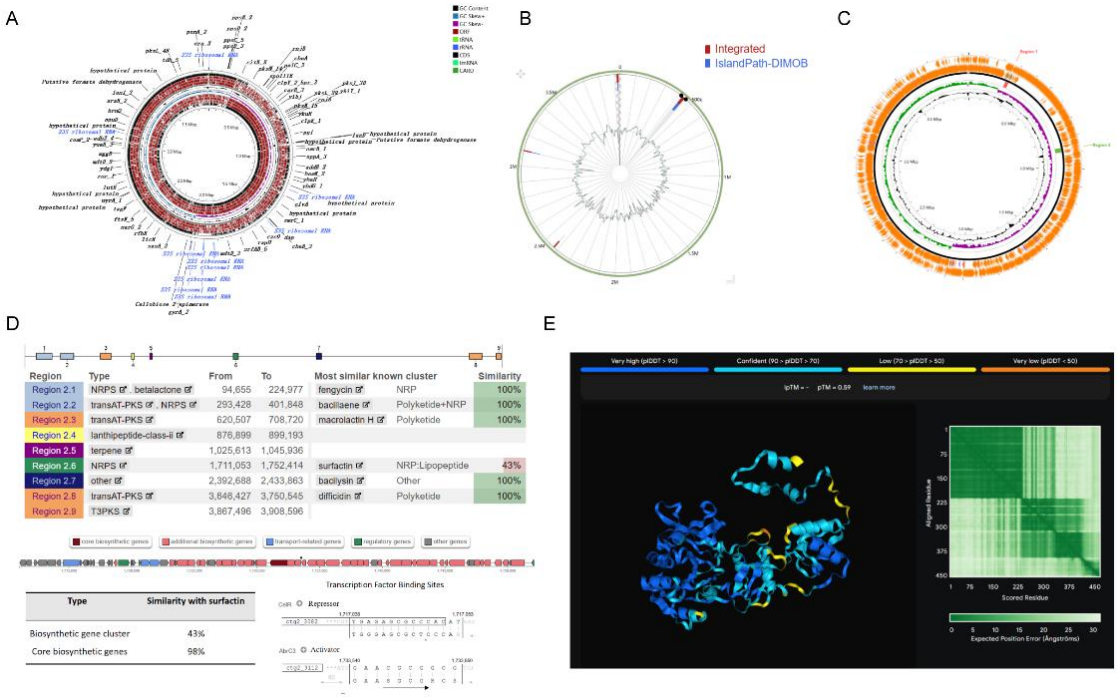

Figure S7. Genomic features and secondary metabolite biosynthetic potential of *Bacillus velezensis* PH3-11. (A) Circular genome map. (B) Genomic island prediction. (C) Prophage prediction. (D) antiSMASH-predicted biosynthetic gene clusters, including a putative surfactin-like BGC showing 43% similarity to a known surfactin cluster. (E) Predicted structure of the core biosynthetic protein from a putative lipopeptide-related BGC.

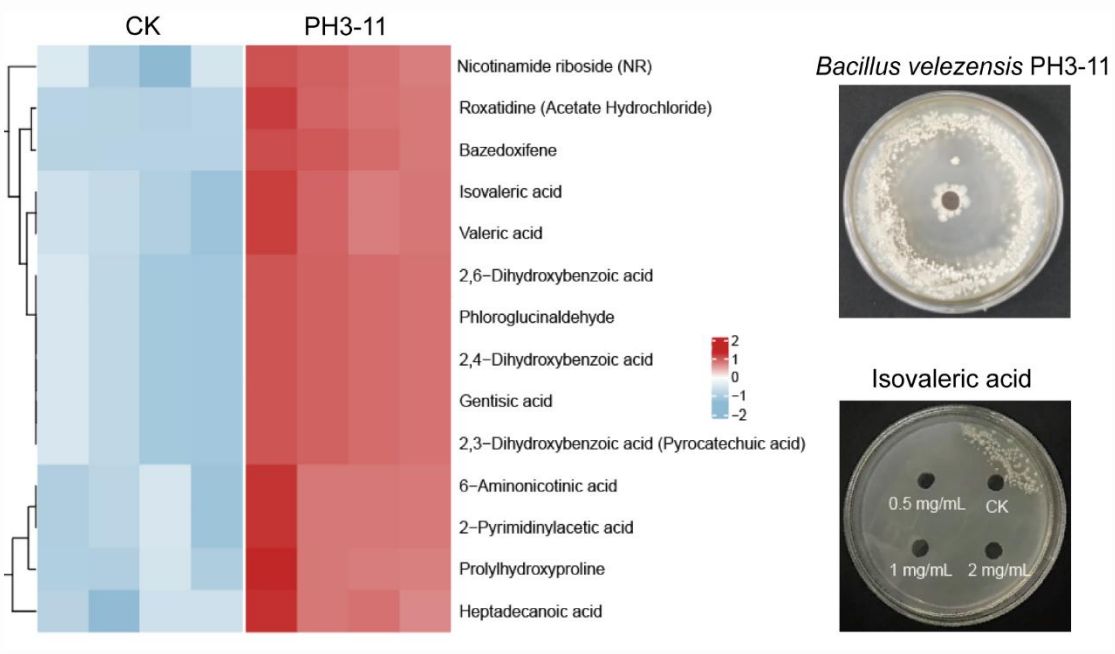

Figure S8. Untargeted metabolomic profiling and functional validation of candidate antimicrobial metabolite produced by *Bacillus velezensis* PH3-11.

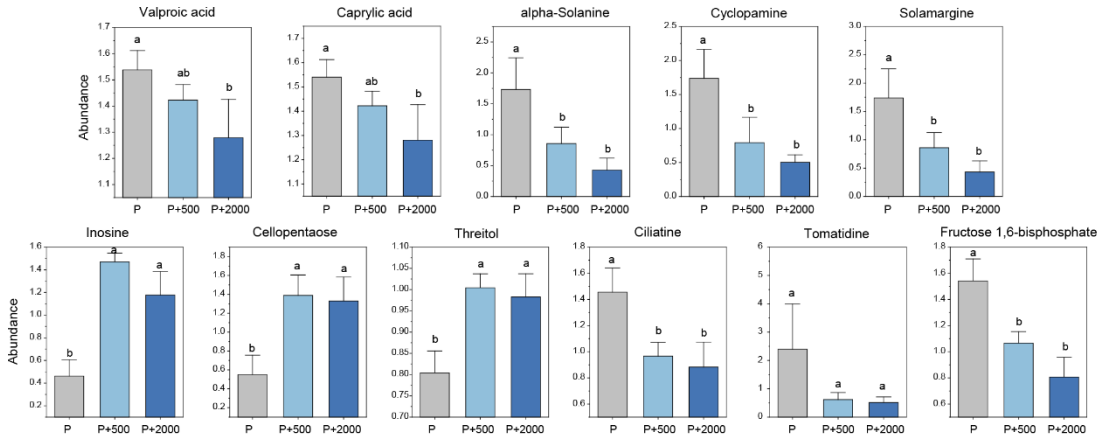

Figure S9. Levels of key soil metabolites associated with SiO_2 NP-responsive biomarker assemblages under different SiO_2 NP treatments. Different letters indicate significant differences among treatments within each subpanel at $P < 0.05$, as determined by one-way ANOVA followed by Duncan's multiple range test.

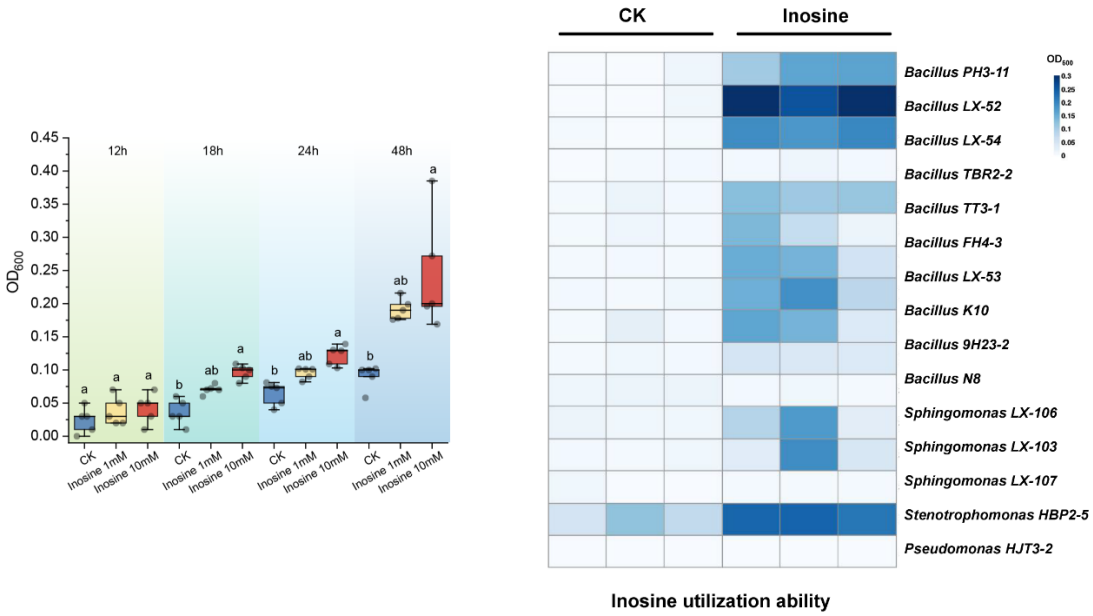

Figure S10. Effects of inosine on the growth of tested bacterial isolates.

Figure S11. Capillary chemotaxis assay showing the chemotactic response of PH3-11 toward inosine *in vitro*. Differences between treatments were assessed using a two-sided Welch's t-test. ***$P < 0.001$.

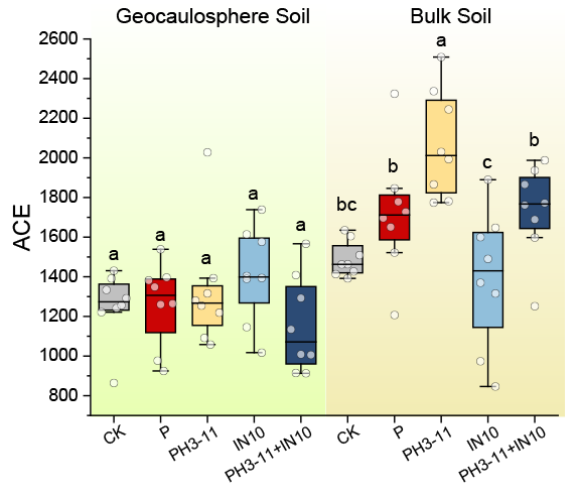

Figure S12. The ACE index of bacterial communities in geocaulosphere soil and bulk soil. Different letters indicate significant differences among treatments within each subpanel at $P < 0.05$, as determined by one-way ANOVA followed by Duncan's multiple range test.

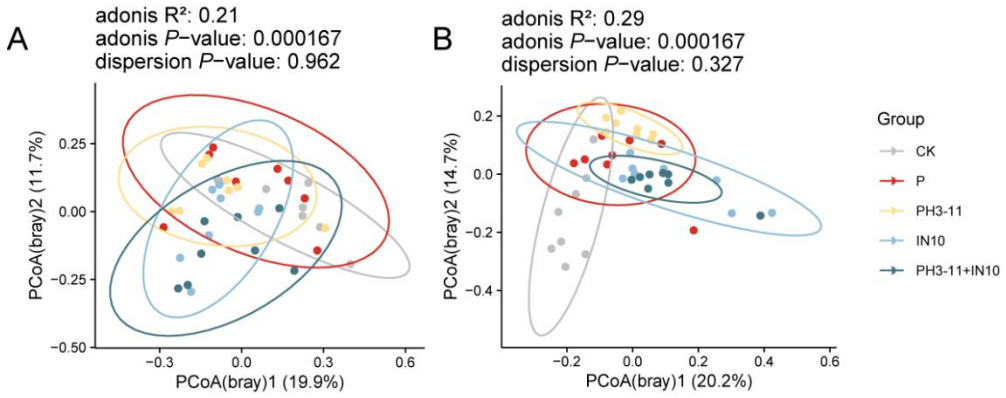

Figure S13. β-diversity of bacterial communities in geocaulosphere soil (A) and bulk soil (B). PCoA was performed based on Bray–Curtis dissimilarity.

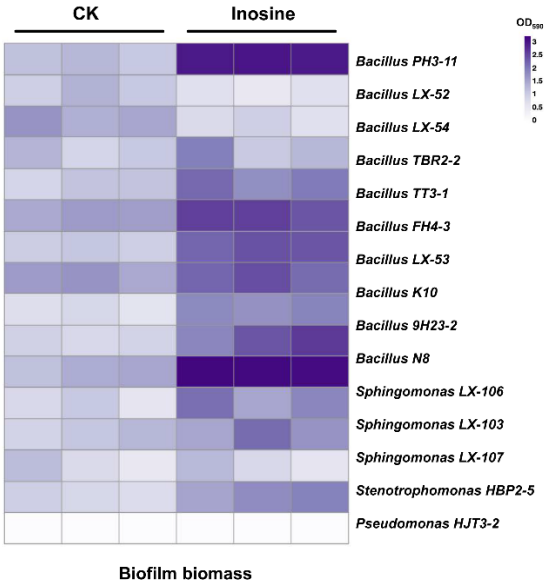

Figure S14. Effect of inosine on biofilm biomass of tested bacterial isolates.

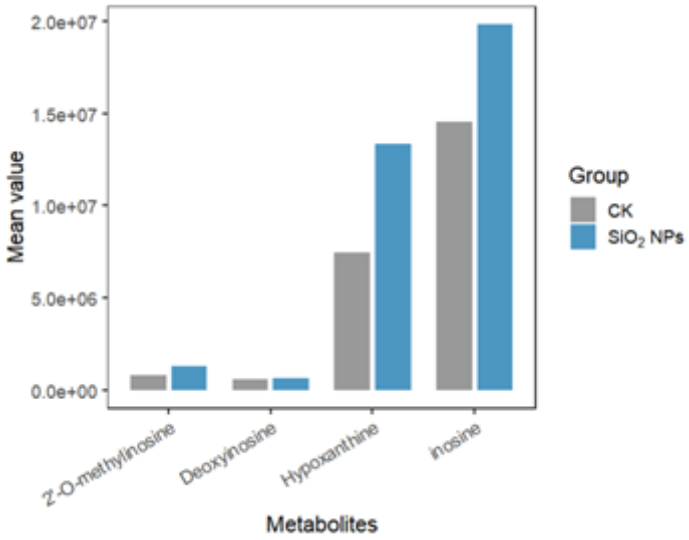

Figure S15. Effects of SiO_2 NPs on the accumulation of inosine and related metabolites in the unplanted soil microcosm.